Fifth International Conference on CFD in the Process Industries
CSIRO, Melbourne, Australia
13-15 December 2006

SWIRL TUBES AS AN IN-LINE GAS-LIQUID SEPARATOR

Pierre Victor CUEILLE [a], Eugênio Spanó ROSA [c]
Gerardo SANCHEZ-SOTO [a], Nabil Noui-MEHIDI [b] and Mayela RIVERO [a]

[a] ARRC, PO Box 1130 Bentley WA 6102, Australia
[b] CMIT, PO Box 56, Highett, Victoria 3190, Australia
[c] UNICAMP, PO Box 6122, Campinas 13083-970, Brazil

ABSTRACT

This work investigates the gas-liquid separation process in swirl tubes also known as in-line separators. They are compact with no moving parts and have low maintenance. These features fit the exigent conditions expected in hostile offshore production environments but so far these devices are not technologically developed to comply with the demands of gas production fields. The goal of this work is to use CFD to investigate the feasibility of these devices as gas-liquid separators.

NOMENCLATURE

D vortex finder diameter
m mass flow rate
X radial coordinate
Y axial coordinate
Z tangential coordinate
U radial velocity
V axial velocity
W tangential velocity
S Swirl number
ρ gas density
ϕ dimensionless mass flow rate

INTRODUCTION

A multiphase flow is likely to occur along production lines found in gas reservoir fields. The fluids produced are mostly gas but the stream may also transport in small concentrations, salt water, oil and sand. The separation of liquids from the gas stream during the initial stages is very desirable. It reduces the well head pressure due only to the transport of gas and increases the well productivity. On the other hand, the separation device has to be simple and reliable with low maintenance requirements and minimal footprint. These constraints make the swirl tube a strong candidate for use under the very exigent conditions expected in hostile offshore production environments.

With reduced size and no moving parts these devices are designed to work in line separating the liquid from the upstream gas flow. The device consists of two concentric pipes which overlap forming a chicane, Fig. 1. Within the annular space between the pipes there are no moving blades to impart a swirl component on the downward liquid stream. The blade flow is discharged at the annular space formed by a chicane or vortex finder, to comply with the nomenclature developed for conical hydrocyclones. At the chicane, the gas stream makes a U turn and is diverted upward toward the production line while the liquid proceed downstream on the external pipe wall to the liquid pipeline.

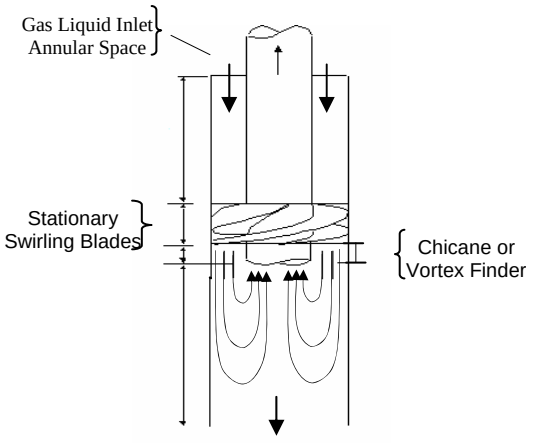

Figure 1: Schematic diagram of the swirl tube.
The present geometry, referred to here as "swirl tubes". It differs from classical centrifugal separation units (GLCC, conical hydrocylone) by its design.

The use of swirl tubes as gas-solid separation devices is already effective but so far there is no reliable model to predict the separation efficiency and further work is necessary, Hoffmann et al. (2002). Their use as gas-liquid separation devices is also known mainly for the purpose of demisting. But there is very little scientific data on this application and no experimental, theoretical or numerical work was found. The presence of liquid droplets and a possible liquid film poses new challenges to the separation phenomena regarding the two phase flow pattern, droplet break-up and coalescence.

This work addresses the understanding of swirl tubes as gas-liquid separator applied to a gas stream with dispersed droplets. The objective of this work is two fold: firstly to characterize the flow field inside the device and secondly to investigate the influence of the increase of swirl numbers on the flow field. Additionally, some estimates of the droplets trajectory will be made using the Lagrangian particle tracking algorithm in a precalculated flow field.

This paper is organized as follows. The numerical method, grid size, convergence criteria and boundary conditions are described in section 2. The flow field analysis is done in section 3 and the Lagrangian particle tracking is shown in section 4. Finally, conclusions are drawn in section 5.

NUMERICAL MODEL

This section presents the numerical method, the grid size, the boundary conditions and the convergence criterion. The mass and momentum equations are solved using the finite volume technique embodied in the ANSYS CFX cfd code. The flow is considered to be in a steady state, incompressible and axis-symmetric. A non-structured mesh is developed to fit the device boundaries. The orthogonal directions are X, Y and Z representing the radial, axial and tangential directions respectively. The flow field has three velocity components: U, V and W, which correspond to the velocities along the X, Y and Z axis. The grid mesh density is proportional to the flow gradients. The number of elements is 200,000 with an average element size of 0.7 mm.

The continuous phase is air. It is considered incompressible and isothermal with transport properties taken at 25°C & 1 atm. The dispersed phase consists of spherical water droplets. The droplet concentration is considered to be low enough as to not disturb the continuous phase flow. The boundary conditions used in this work are: mass and momentum inflow at the inlet, no-slip at the external and bottom walls, periodic flow along the Z direction, flow symmetry at the centerline and at the outlet the flow is locally parabolic. The mass and momentum inlet flows are defined in terms of the inlet axial velocity, V_{in}, and the Swirl number is defined as:

$$S = W_{in} / V_{in} , \qquad (1)$$

where Win represents the inlet tangential velocity. This velocity is set by the inclination of the blades trailing edge.

The flow regime is turbulent. The Reynolds number is in the order of 10^4 based on the inlet size. A short survey of the grid sensibility showed that a good compromise between runtimes and numerical accuracy was achieved with the mesh described above. The mesh is inflated near solid boundaries to assure a minimum distance from nearest node to the wall of 5 wall units.

The advection scheme survey showed the High Resolution scheme generates numerical instabilities, observable in the radial velocity profile,. A change for the Upwind scheme was also chosen in order to focus on the main physical phenomena. To help the convergence, in this case of wall-bounded turbulent flow, the momentum equations were solved using the k-ω turbulence model with low Reynolds capability. This approach automatically considers a specific set of modified k-omega equations to make the resolution in the boundary layer.

The numerical solution is stopped when the sum, over all control volumes, of the RMS residuals of the mass and the momentum equations falls below 10^{-6}, which corresponds to less than 0.005% of imbalance for each equation.

RESULTS

Three numerical flow simulations were performed. All of them have the same inlet axial velocity of 9 m/s but distinct swirl numbers of 0, 1 and 5. The swirl equal to zero means a case with no tangential velocity. It is a useful standard to draw comparisons of the swirl effect with the flow. The CFD results are presented in the following two sub-sections: the first describes the flow field and the second explores the effects of increasing the swirl number.

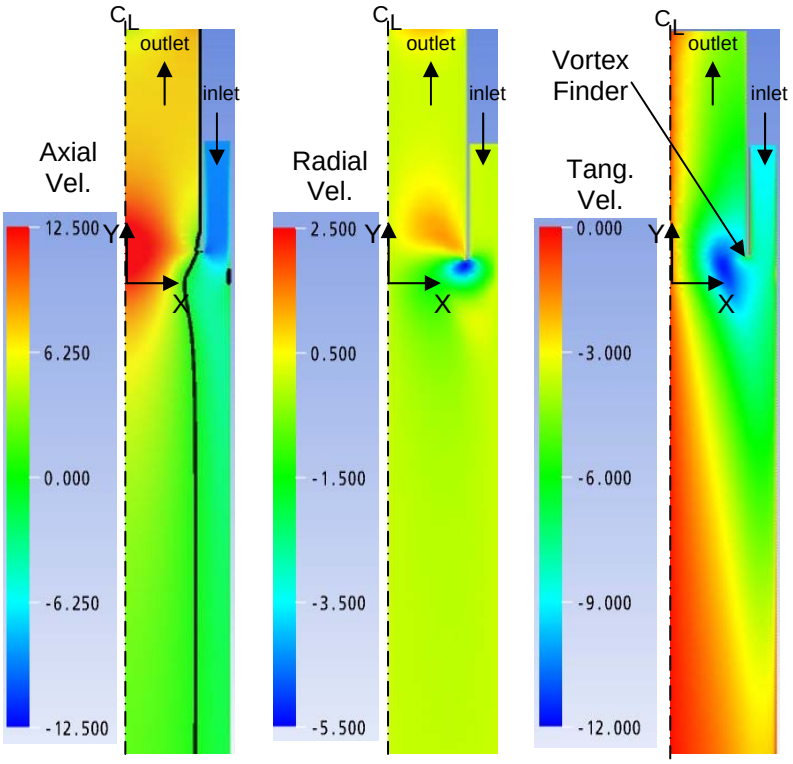

Figure 2: Velocity fields for the axial, radial and tangential velocity components

Flow Field Description

The flow field description is done for a case where the inlet velocity is 9m/s with a swirl number of 1. A colour map of the axial, radial and tangential velocities is shown in Fig. 2. The dash-dotted line represents the device

centre-line. The axial velocity is primarily described by one descendent stream and an upward stream, i.e. a reversed flow. The locus of null axial velocity is represented by the continuous black line on the map. It is nearly concurrent with the radial position of the vortex finder wall and also agrees with experimental evidence in cone-cylindrical cyclones as well as in swirl tubes (Peng. et. all 2002). For a constant Y section, V exhibits a local maximum at the centre-line. It also decays as the distance from the vortex finder increases downward. The flow at the inlet has to do a U turn to exit the domain through the outlet. This happens due to the radial velocity transport. Underneath the vortex finder there is a region with strong inward velocity (negative values of U). It is responsible for the majority of mass transport from the downward stream flow to the upward stream. Finally the tangential velocity also displays its highest values underneath the vortex finder. Near the pipe centreline it is null. The tangential velocity also decays as the distance from the vortex finder increases downward.

Swirl Number Effect

The separation process for a droplet inside the swirl tube is described qualitatively as follows. The droplets discharged at the blades' trailing edge possess tangential and axial velocity components. The tangential component generates a centrifugal force pushing the droplets against the outer wall. The axial velocity is always downward at the region between the vortex finder and the outer wall. Therefore these two velocities are not capable of displacing the droplet inward or causing the droplet to carry over. Ultimately it is the upward gas stream which carries the droplet, but it is necessary to have the inward transport given by the radial velocity field. For this reason the radial velocity field is the main influence on the separation efficiency. The inward and upward droplet transport only happens when the inward and upward gas velocity fields are higher than the droplet terminal velocity due to the centrifugal and gravitational force fields.

Targeting the swirl tube separation efficiency, a good design would require a radial velocity profile displaying no peaking values for the inward velocities. This feature would avoid local regions with high inward velocities capable of transporting the droplet.

Inward radial velocity profiles without peaking values are hard to produce as the flow has a natural tendency to exhibit maximum inward velocity just underneath the vortex finder. The purpose of this section is to investigate the sensitivity of the radial velocity profile as the swirl number increases.

The radial velocity profile is taken at the surface A-A as shown in Fig. 3. This surface is just an extension of the vortex finder wall. It coincides with the null axial velocity locus, as seen on Fig. 2, due to continuity, the entire inlet mass flow rate has to cross A-A.

Figure 4 displays the radial velocity U as a function of the axial distance of the vortex finder expressed in terms of its diameter D. The inset on Fig 4 shows a magnified area on the vertical axis. The curves represent data from swirl 0, 1 and 5 with an axial velocity of 9 m/s. The vortex finder wall is positioned at the origin of the coordinate system. As one moves away from the vortex finder the value of the inward velocity increases to a maximum. The swirl 0 curve experiences the highest inward velocity peak which is at -8.5 m/s. As the swirl number increases from zero to 1 the peak value decreases to nearly -4 m/s and disappears at S=5. Moving further away, the inward velocity decreases. For the S=0 and S=1 curves, the observed outward velocity is in accordance with the experimental observations of Peng et al., 2002, but not for the S=5 curve. The existence of an outward velocity is associated with a secondary flow cell produced by the intense inward velocity below the vortex finder. After this region the radial velocity decreases slowly approaching zero. The decay rate depends on the swirl number but at a distance of 5D they are one order of magnitude less than the inward peak values. As observed in Fig. 4, an increase in the swirl number decreases the inward velocity peak which may enhance the separation efficiency.

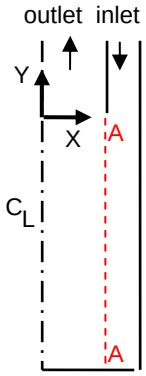

Figure 3: A-A displays the surface where the radial velocity U is taken.

Figure 5 complements the information shown in Fig. 4 as it represents the dimensionless mass flow rate crossing the A-A surface and is defined as:

$$\phi = \frac{\int_{Y_{ini}}^{Y} \rho \cdot U \cdot \pi D \cdot dY}{\dot{m}_{inlet}}, \qquad (2)$$

where Y represents the axial distance measured from the vortex finder, m_{inlet} is the inlet mass flow rate, ρ is the air density and U the radial velocity. ϕ represents the dimensionless cumulative mass flow rate crossing the A-A surface, within the interval of $0 \le \phi \le 1$.

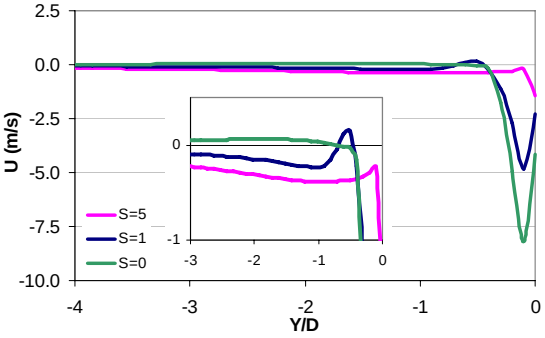

Figure 4: Radial velocity profile at the A-A surface as a function of the axial distance.

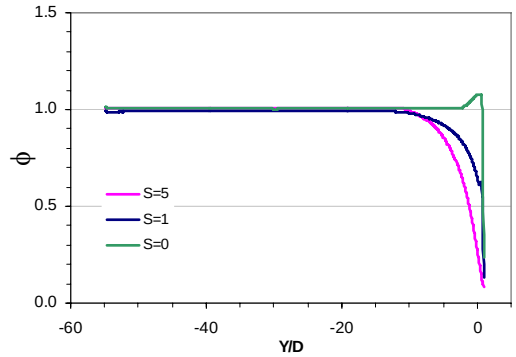

Figure 5: Dimensionless mass flow rate crossing the A-A surface as a function of the axial distance.

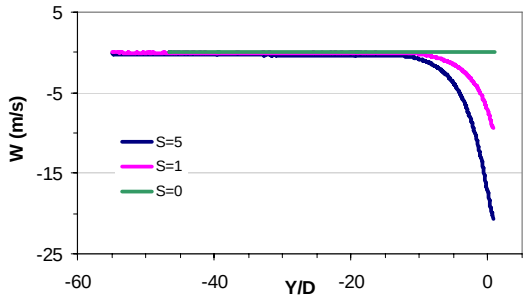

Figure 6: Tangential velocity profile at A-A surface as a function of the axial distance.

The swirl zero case has most of its downward mass flow transferred to the upward stream in less than 1D, as shown in Fig. 5. Due to this fast inward moving stream it forms a recirculation cell which is responsible for ϕ values greater than one. On the other hand, for the S=1 and S=5 curves the growth rate of ϕ is relatively slower if compared to the S=0 case. Just below the vortex finder the initial values of ϕ are around 0.1 but it requires a distance of 7D and 13D to achieve 97% of the inlet mass flow when S=1 and S=5, respectively. This distance can also be considered representative of the decaying length of the axial and tangential velocity fields. Figure 5 is also a test for the overall mass flow balance. For large values of Y/D, ϕ must approach unity indicating that the entire inlet mass flow rate has already crossed the A-A surface. In fact at a distance of 55D below the vortex finder the ϕ values are within 0.99 and 1.01 for all the swirl numbers.

Finally, Figure 6 displays the tangential velocity as a function of the axial distance from the vortex finder expressed in terms of its diameter. This figure displays the decaying of the tangential velocity for swirl numbers 1 and 5. Obviously S=0 has no swirl and as such is just used as a reference. The swirling velocity does decay as the axial velocity. Increasing the swirl number from 1 to 5 will decrease the tangential velocity decaying length but not significantly.

DROPLETS TRAJECTORIES

The assessment of the swirl tube separator performance is completed by comparing the droplet trajectories when the swirl number increases from 0 to 5. The main assumption is that the droplet concentration is low enough so that they do not interfere with the gas continuous phase flow. The particles trajectories are evaluated using the Lagrangian tracking algorithm embodied in ANSYS CFX. Droplet acceleration results from the drag, pressure and virtual mass forces acting on it. Individual 5μm diameter spherical droplets of water are considered to have a representative size resulting from the breakup process due to atomization at the blades. They are released from the

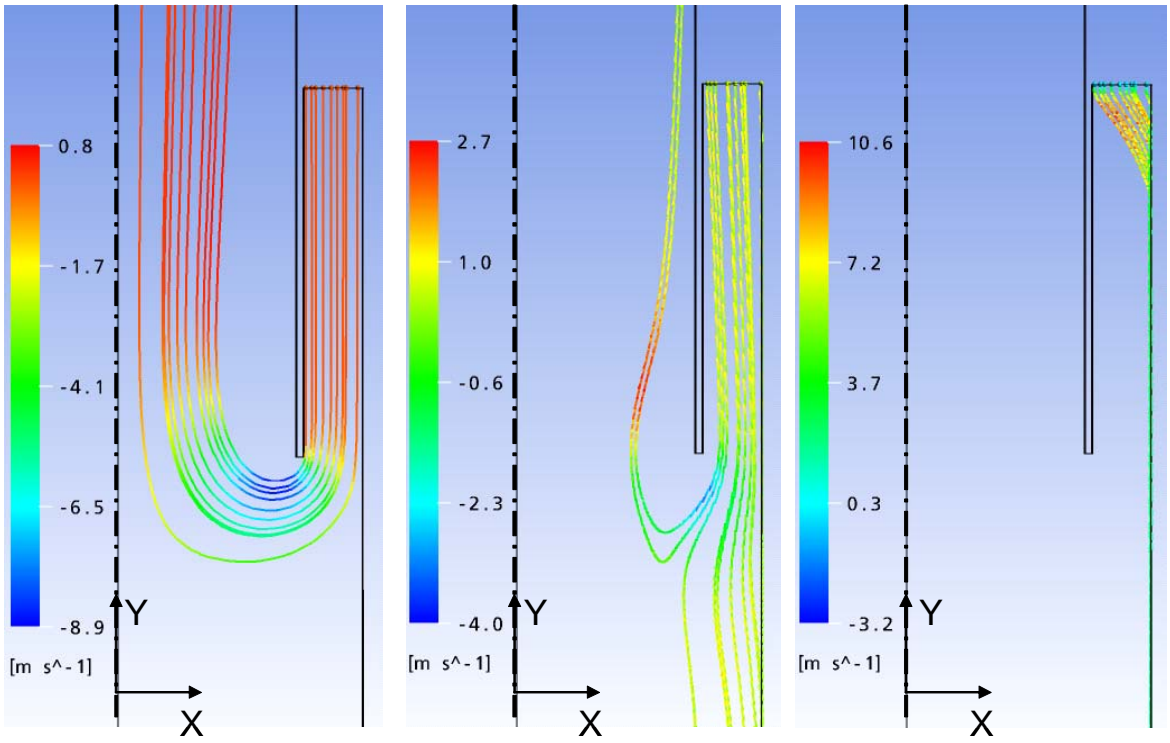

Figure 7: 5μm droplets trajectories for swirl numbers, from left to right respectively, of 0, 1 and 5. The colour scale represents the radial velocity at the droplet position.

inlet with uniform concentration throughout the inlet area. The droplets initial axial and tangential velocities are coincidental with the inlet gas velocities. The droplets trajectories for swirl numbers, from left to right respectively, of 0, 1 and 5 are shown in Figure 7. The colour scale represents the radial velocity at the droplet position.

As seen in Figure 7, the swirl zero example has all droplets being carried over. The swirl number 1 has nearly 15% of the inlet droplets being carried over. Finally the swirl number 5 does not exhibit any droplet carry over. It has such a strong centrifugal force field that all the droplets migrate to the outer wall before exiting the chicane.

Experimental, investigations conducted on swirl tubes of similar size showed a strong reduction of liquid carry over with increasing Swirl number. However, quantitative predictions will demand a model tunning in order to match the droplets size and experimental liquid carry over. It is expected that these issues can be addressed with better modelling including stochastic capabilities in future work.

CONCLUSION

The flow within the swirl tube is characterized by two axial streams with opposite flow directions, downward near the wall and upward at the pipe core. The null axial velocity zone within this shear layer practically coincides with the position of the surface extending from the vortex finder wall into the flow domain. The mass is transferred from the downward stream to the upward stream due to the radial velocity field. An inward velocity peak is observed just below the vortex finder inlet. Its existence is related to the swirl number. The highest inward peak is observed for zero swirl flow. Increasing of the swirl number leads to a decrease in the inward peak velocity. The impact of the increase in the swirl number on a dilute dispersed 5μm water droplet flow was assessed by the Lagrangian particle transport model. The undesirable droplet upward transport, or droplet carry-over, decreases as the swirl number increases. The estimated percentage of droplets carried over were 100%, 15% and 0% when the swirl number increased from 0 to 1 to 5, respectively.

REFERENCES

HOFFMMANN, A.C. and STEIN, L.E., 2002, “Gas Cyclones and Swirl Tubes: Principles, Design and and Operation”, Springer-Verlag.

PENG, W. , A.C. Hofmann, P.J.A.J. BOOT, A. UDDING, H.W.A. DRIES, A. EKTER and J. KATER 2002, “Flow pattern in reverse-flow centrifugal separators”, *Powder Technology”*, **127,** 212-222.